

Fracture Toughness Tests of Structural Weldments


by

Breanna M. Weir

Submitted to the
Office of Honors Programs and Academic Scholarships
Texas A&M University
in partial fulfillment of the requirements for the
1998-99 UNIVERSITY UNDERGRADUATE RESEARCH FELLOWS PROGRAM

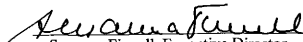
April 15, 1999

Approved as to style and content by:



Gary T. Fry

Department of Civil Engineering



Susanna Finnell, Executive Director
Honors Programs and Academic Scholarships

Engineering Group II

Abstract

Insuring structural integrity demands an ever-increasing understanding of material behavior. While engineers have long agreed on methods for measuring the strength or elasticity of a material, such a consensus has yet to be reached on the determination of fracture toughness.

Fracture toughness measures material resistance to the presence of a crack or other flaw. Low fracture toughness indicates brittle behavior if a flaw is present. One way to quantify fracture toughness uses crack-tip opening displacement (CTOD).

The American Society for Testing and Materials has recently proposed an annex to ASTM E1290-93 revising the current CTOD standard specifically for weld use. This paper focuses on the application of the ASTM annex to steel bend specimens and an analysis of its efficacy in terms of reproducibility, temperature variation, similarity to E1290, and procedural success.

The annex demonstrates reliability in its calculation of critical CTOD values. It also appears theoretically sound. Including this addendum in the E1290 standard is endorsed.

Table of Contents

1. Abstract	i
2. Introduction	
<i>Background Material</i>	1
<i>Literature Review</i>	5
3. Procedures	
<i>Standard Comparison</i>	14
<i>Single Edge Notched Bend Specimens</i>	15
4. Results	19
5. Discussion	20
6. Conclusions	23
7. Acknowledgements	25
8. References	26
9. Tables	
<i>Table One: Specimen Dimensions</i>	32
<i>Table Two: Material Properties</i>	32
<i>Table Three: Crack Straightness Data</i>	33
<i>Table Four: Critical Fracture Toughness Data</i>	33
10. Figures	
<i>Figure One: Crack-Tip Opening Displacement Definition</i>	34
<i>Figure Two: Similar Triangles Analysis</i>	35
<i>Figure Three: Specimen Configurations</i>	36

<i>Figure Four: Compression Fixture</i>	37
<i>Figure Five: Straight vs. Realistic Crack Faces</i>	38
<i>Figure Six: Schematic of Specimen Loading</i>	39
<i>Figure Seven: Single Edge Notch Bend Tests</i>	40
<i>Figure Eight: R2-1 Results</i>	41
<i>Figure Nine: C14-1 Results</i>	42
<i>Figure Ten: R2-4 Results</i>	43
<i>Figure Eleven: L15-4 Results</i>	44
11) Appendix I: Derivation of Equations	45

Fracture Toughness Tests of Structural Weldments

The American Society for Testing and Materials is responsible for researching, publishing, and updating technical standards that affect almost every aspect of daily life. With this diversity comes a responsibility to ensure the quality and accuracy of the work to which the society attaches its name. Once adopted, a standard becomes part of the fabric of industry and research alike. The proposal of a new standard, or the modification of an old one, is therefore a weighty event.

An annex to current standard ASTM E1290-93 lies before the society. The proposed annex targets fracture toughness measurements in welded specimens removed from structural components.

Should the E1290 annex be accepted for use? This simple question forces much deeper considerations. Fracture toughness is an elusive property that fascinates and frustrates, yet it remains a critical element in understanding material behavior. Ensuring the safety of critical structural weldments requires a rigorous definition of fracture toughness. Through a theoretical and experimental examination of the E1290 annex, this paper strives to establish a better definition of fracture toughness as well as the validity of the proposed annex.

Background Material

Fracture mechanics is a relatively new discipline concerned with understanding the why and how of material fracture. “The ultimate aim of fracture mechanics is fracture control... to develop procedures for controlling fracture in practical engineering components” (Rooke 1994). Failure of an individual component often leads to failure of

the structure as a whole. The search for logic behind fracture has led to the magnifying glass and a careful examination of component integrity. Researchers now believe that the fracture of engineering structures is usually caused by the initiation of cracks, or crack-like flaws and defects, which propagate until reaching a critical size (Imhof and Barsom 1973). At the point of critical crack extension, the structure fails.

Simply eliminating cracks, or flaws that could lead to cracks, is an untenable solution. Any large, complex structure contains sharp discontinuities or flaws of some type (Bucci, Greene, and Paris 1973). Cracks and defects are a reality which must be dealt with rather than an annoyance to be eliminated. Therefore, the success of structural projects necessitates an understanding of the influence on material behavior held by these imperfections (Bucci, Greene, and Paris 1973).

Fracture mechanics uses various parameters to classify and interpret material behavior in order to understand issues of component life or critical crack dimensions (Bucci, Greene, and Paris 1973). One of these parameters is fracture toughness.

Fracture toughness quantifies the resistance of a material to physical separation through crack propagation (Sih 1976). Most engineers will classify a material as either ductile or brittle. However, even a ductile material may behave brittly in the presence of a crack or other flaw such as may be generated in the construction process. A tough material remains ductile even when cracked. The higher the fracture toughness, the less sensitive the material to flaws.

Several measurements of fracture toughness have been proposed. ASTM standard E1290 and its annex deal with the calculation of crack-tip-opening displacement (CTOD). CTOD measures how blunt a crack becomes before propagating. According to a 1976

description by Begley and Landes, the process of fracture begins with a very sharp crack, previously introduced by fatigue loads, in an unloaded specimen. As the specimen is loaded, the crack begins to blunt. Blunting increases with load until reaching a critical value of load, at which the crack advances ahead of the blunted tip (Begley and Landes 1976). The blunter the crack, the tougher the material being tested (Anderson 1995). CTOD is measured from two specific points along the crack face, as shown in the schematic drawing of Figure One.

CTOD is a particularly useful measurement of fracture toughness because it models a physical quantity. A small crack may be integrated into a finite element model and used to determine the required CTOD for a structural component in a given scenario. CTOD may even be directly measured in test specimens with crack-tip molds created from silicon rubber, a dental impression material (Robinson and Tetelman 1974).

Fracture toughness aids in material selection, welding procedure quality checks, and fitness-for-purpose analyses (Dawes, Pisarski, and Squirrel 1989). This parameter holds special importance in dealing with welded constituents. Because of the material heterogeneity and residual stresses present in welds, the application of fracture toughness is still a complex problem (Sih 1976). Inclusions and incomplete fusion also complicate weldment analysis (Glinka 1977). Using the K parameter, a popular measure of fracture toughness, it is not even possible to get toughness measurements for many welds (Nelson and Kaufman 1973). Weld metal toughness may depend on the welding process, base metal composition, joint thickness, preheat or interpass temperatures, post-weld heat treatments, and other variables (Dawes, Pisarski, and Squirrel 1989). Weldments are considered more susceptible to fatigue failure than base material (Glinka 1979).

The importance of weld metal toughness was illustrated in the earthquakes that struck Northridge, California, in 1994 and Kobe, Japan, in 1995. During these earthquakes, hundreds of girder-column buildings failed. In these buildings, tall columns form skeleton walls of a building and long girders serve as floors. The girder consists of an “I”-shaped piece of steel, the center of which is called the web. The horizontal sections, on the top and bottom of the “I,” are known as flanges. The girder flanges are welded to the columns.

The weldments at the girder-column contact were designed to deform elastically in moderate earthquakes and plastically in severe shaking (Iwankiew and Carter 1996). This ductility allows the structure to deform while preserving the ninety-degree angle between floor and wall, thus ensuring the safety of those inside and reducing damage to the building.

Earthquake failure resulted from fractures, which severed the connecting weldments between the flanges and the column (Xue et al 1996). In a few cases, the affected structures collapsed entirely. The failure of the girder-column buildings stunned the industry. Structures which were “once thought safe because of steel’s inherent ability to absorb energy by deforming [suddenly became] a surprising new threat” (Normile 1996). Post-quake study revealed that the cracks causing failure originated near the seams of the girder-column weld. Not only did the weldments fail at lower than expected yield strengths, but the material also failed in a brittle manner (Xue et al 1996).

In the aftermath of the earthquakes, some engineers initially attributed the failures to lack of weld metal ductility, thus accounting for the brittle fractures (“Magnitude”

1994). However, later investigations suggest the failures stemmed from an overloaded joint detail with poor local fracture resistance (Joh and Chen 1997).

Clearly, fracture toughness is an important variable in determining material suitability. Just as a chain is only as strong as its weakest link, a structure is only as tough as its most brittle member. Continued use of poor toughness material provides continued opportunity for failures of the magnitude seen in California and Japan.

Literature Review

The main impetus for the development of fracture toughness as a quantifiable parameter stemmed from structural failures during and after World War II.

Prior to this date, little was known about brittle fracture, although problems with “mysterious cracking of steel in a brittle manner” were recorded as early as the late 19th century by British Iron and Steel Institute reports (Rolfe and Barsom 1977). Although this was the earliest recorded instance of failure, it was not to be the last. Catastrophic failures were recorded for gas holders, water tanks, and oil tanks in the early years of this century (Rolfe and Barsom 1977).

In January 1919, a tank holding 2.3 million gallons of molasses ruptured in what was to become one of the most famous cases of brittle failure; Rolfe and Barsom’s text details this incident. The molasses drowned twelve people, seriously injured forty others, damaged houses, knocked over a portion of the Boston Elevated Railway, and drowned several horses. The ensuing lawsuit spanned years and called upon the testimony of leading engineers and scientists of the day. The court-appointed auditor best summarized the limited understanding of brittle fracture when he wrote: “...the auditor has at times felt that the only rock to which he could safely cling was the obvious fact that at least one half

of the scientists must be wrong.” Eventually, the auditor reported that the failure was due to “overstress.”

Such was the status of fracture research prior to World War II. However, the failure of several important military structures during the war helped bring new interest to the field of fracture mechanics (Anderson 1995). Among these incidents ranked the failure of welded Liberty Ships and T-2 tankers. The T-2 tankers displayed fractures originating in defects of the bottom-shell butt welds; however, the failures of these ships, nine of which split in two during service, could also be partially accounted for by poor steel quality (Barsome and Rolfe 1977). The Liberty ships were built from a poor fracture toughness steel and exhibited local stress concentrations in the hatch corners; these factors allowed crack-like flaws in the welds to propagate and, in some cases, sever the hull of the ship (Anderson 1995).

Failures occurring in gasoline transmission lines, oil-storage tanks, and pressurized cabin planes also brought interest to the field of fracture mechanics (Irwin 1957). A “prominent feature” of these failures was the propagation of a brittle crack across components with an average tensile load “safely below” the material’s yield strength (Irwin 1957).

The avoidance of future disasters dictated a better understanding of fracture mechanics. This call for new understanding led to a “revival of interest” in the Griffith theory of fracture strength (Irwin 1957).

In 1920, A. A. Griffith conducted a series of experiments on glass rods. To explain the different tensile strengths associated with similarly sized rods, Griffith postulated the existence of crack-like flaws capable of growing under loads (Rooke 1994).

Griffith suggested that crack growth was controlled by a balance between the strain energy and the energy needed to form new crack surfaces; when it took more work to resist deformation than to form new surfaces, the crack would propagate (Rooke 1994). He developed a way of modeling this behavior mathematically and successfully used it to model behavior in the glass rods (Anderson 1995).

In the wake of the World War II failures, two independent papers, written by G. R. Irwin in 1948 and E. Orowan in 1952, called for the use of a modified Griffith theory in understanding the development of rapid fracture (Irwin 1957). Irwin and Orowan extended Griffith's theory to ductile metals by suggesting an energy of deformation term, since this quantity can be larger than the surface (or strain) energy in ductile metals (Rooke 1994). Since the non-recoverable work associated with permanent deformation is much greater than the work required to form new crack surfaces in ductile metals, Irwin and Orowan both postulated that cracks would propagate in metal when the applied strain energy was greater than the work of deformation (Rooke 1994). This hypothesis explained why ductile materials are harder to break than brittle materials, such as glass. Materials with a large work of deformation began to be called "tough," which led to the term "fracture toughness" (Rooke 1994).

Later, working with the Naval Research Laboratory as superintendent of the Mechanics Division, Irwin further expanded the field of fracture mechanics (Anderson 1995). Irwin showed that the elastic stress near a crack tip depended on spatial coordinates and that stress magnitude could be determined by a stress intensity factor, which related to Griffith's strain energy term (Rooke 1994). This research brought the stress concentration factor, K , into successful use in the field (Anderson 1995).

In 1961, A. A. Wells proposed a new measure of fracture toughness which he called crack-tip opening displacement (CTOD) (Shih 1981). CTOD describes the capacity of a material near the crack tip to deform before crack extension (Shang-Xian 1983).

Initially, there was some dispute as to how CTOD should be measured. A small-scale yield model by Wells and a strip yield model by D. S. Dugdale were both used to characterize CTOD (Dawes 1977). Dugdale's analysis considered the effects of notches and slits on material; the main focus was to model the extent of material yielding as a function of external load (Dugdale 1959). At the time of this analysis, Wells would not introduce CTOD for another two years. However, early CTOD researchers used Dugdale's model as well as Wells's to assume that CTOD occurred at the original crack-tip as well as the elastic plastic boundary, which implied a square "nose" in the crack-tip profile (Dawes 1977). Rice and Johnson, in a 1970 paper, predicted the crack-tip would deform radially; this prediction was born out with physical experiments (Dawes 1977). After some further debate on the shape of crack profiles, a definition of CTOD based on the displacement of the crack-tip came into use; this neglected crack profiles and minimized ambiguity caused by the geometric debate (Dawes 1977).

Engineers in the United Kingdom used CTOD in developing oil resources in the North Sea (Anderson 1995). The Welding Institute is credited with "pioneering" the use of CTOD by developing the CTOD design curve (Harrison et al. 1977). In 1966, F. M. Burdekin and D. E. W. Stone established a basis for this curve by extending the Dugdale and Wells models (Harrison et al. 1977). Later, the basis for the CTOD design curve was refined to incorporate new findings and put in final form by Dawes (Harrison et al. 1977).

The development of the J contour integral as a fracture toughness barometer ran parallel to the CTOD evolution.

J. R. Rice published his work on the J integral in 1968 (Rice 1968). Like Griffith's work, the J integral initially seemed doomed to obscurity, despite a simultaneous and independent derivation by J. D. Eshelby (Anderson 1995). Eshelby was the first to associate the force on an elastic defect with a conservative integral quantifiable over the defect's surrounding surface (Rice 1985). In 1968, Eshelby published accounts detailing the calculation of forces acting on static and moving cracks in elastic media using the elastic energy momentum tensor (Bilby 1985). Rice's publication put forth similar work on the momentum tensor; however, unlike Eshelby's derivation, Rice's integral was applicable to both elastic and plastic media (Bilby 1985).

With these publications, Griffith's strain energy term became synonymous with the J integral near the crack tip; the J integral, instead of being an energy release rate, became a parameter characterizing the intensity of the near-tip crack deformation field (Rice 1985). In other words, the J integral became a measure of fracture toughness. However, it was not immediately accepted as such, and the stress concentration factor, K , continued to dominate toughness assessments.

The American nuclear power industry's interest in the fracture of nuclear pressure vessels kept fracture mechanics research alive after the initial lack of enthusiasm for the J integral (Anderson 1995). In 1971, J. A. Begley and J. D. Landes rediscovered Rice's work and successfully characterized fracture toughness for these pressure vessels (Anderson 1995). Experimental investigations by Begley and Landes (1972) and Green

and Knot (1975) went on to show that a critical J integral value or critical crack opening displacement may be used to characterize the onset of crack growth (Shih 1981).

In 1971, several researchers began a concerted effort to bring the J integral into more extensive use. Sighting that the “as yet relatively unexplored” J integral could be as easy to use as the popular K parameter, a team of Rice, P. C. Paris, and J. G. Merkle introduced new J estimation formulas based on common specimen geometry (Rice, Paris, and Merkle 1973). Begley and Landes championed the J integral as a method of expanding linear elastic fracture mechanics, which only allows for analysis of plastic behavior on a small scale, to cases with large scale plasticity (Begley and Landes 1973). The J integral is an average measurement of the crack-tip elastic-plastic field and can be evaluated experimentally (Begley and Landes 1971). It was a parameter that used crack initiation as a toughness measurement but did not require any numerical techniques to model near crack-tip behavior, an advantage over CTOD since little could actually be observed of the crack-tip (Begley and Landes 1971). This lack of numerical dependence, along with its applicability to elastic and plastic media, made the J integral worth noting.

From this point, acceptance and use of the J integral and CTOD began to blend as engineers struggled to define a quintessential measurement of fracture toughness.

In 1979, J. W. Hutchinson and Paris began to argue that the J integral was a valid measure of the strength of the stress and strain fields surrounding the crack growth zone (Shih 1981). From the idea of characterizing the point at which a crack begins to grow came the idea of using the J integral and other parameters as a measure of a material’s resistance to crack growth. This concept enabled a team of Paris, H. Tada, H. Ernst, and A. Zahoor to propose a procedure for measuring crack instability that relied on the J

integral's characterization of fracture toughness (Paris et al. 1977). However, Dawes noted that application of the J integral was problematic when cracks occurred in weld regions and often resulted in toughness overestimation (Dawes 1977).

In 1976, C. F. Shih and Hutchinson established a relationship between toughness, stress, and flaw size (Anderson 1995). This relationship was considered accurate for applied loads, crack-opening displacements, the J integral, and load point displacement (Shih and Hutchinson 1976). Shih and Hutchinson's analysis led to the publication of ASTM 813-81, a standard for J integral testing (Anderson 1995).

As early as 1971, Paris had noted a linear relationship between CTOD and the J integral (Begley and Landes 1971). In fact, Begley and Landes considered this relationship in later J integral development; they obtained a linear relationship between J and a term they called "degree of blunting" (Begley and Landes 1971). Dawes suggested a "close mathematical link" between J and CTOD and suggested that both were equally useful as fracture toughness parameters (Dawes 1977). However, CTOD and the J integral did not formally come together until 1981, when Shih continued his previous research on toughness relationships. Shih first asserted that the crack opening angle remains essentially constant during crack extension, and that CTOD can be used as a measure of material resistance (Shih 1981). Then, examining CTOD and the J integral, Shih concluded that a unique relationship existed between the two parameters for work hardened materials; this finding was corroborated with finite element analysis (Shih 1981). The relationship between J and CTOD allowed for the creation of ASTM E1290 in 1990.

Problems with the E1290 standard, however, were soon in coming. In fact, before standard publication, it was noted that residual stresses caused uneven crack growth,

especially in welds, and that these stresses could be relieved by compression (Dawes, Pisanski, and Squirrel 1989). This fact was not incorporated into the E1290 testing procedure.

In 1992, M. T. Kirk and R. H. Dodds began to consider the plastic portion of the J integral. Finite element analysis revealed error in the E1290 calculation (Kirk and Dodds 1992). Kirk and Dodds later “revealed a fundamental limitation” to E1290 by pointing out that the standard assumes a linear proportionality between CTOD and crack-mouth opening displacement (CMOD) (Kirk and Wang 1995). The pair illustrated that this proportionality breaks down for work hardened materials and, in fact, allows a 25% overestimation in toughness calculations (Kirk and Wang 1995). Kirk and Dodds proposed a new method of calculating the plastic J integral using the plastic work required for CMOD (Kirk and Dodds 1993). They also proposed measuring CMOD instead of back calculating the values from limit load displacements, which simplified the testing procedure (Kirk and Dodds 1993). Kirk and Wang further refined the E1290 calculations by developing empirical equations to determine necessary constants, via finite element analysis and data fitting (Kirk and Wang 1995).

It is interesting to note that the plastic work term introduced by Kirk and Dodds was, in fact, a generalization of Rice, Paris, and Merkle’s estimation formulas based on specimen geometry (Rice, Paris, and Merkle 1973). However, the earlier estimation was meant as a “rapid, inexpensive screening test” and not a general method for measuring material resistance to crack extension (Underwood 1978). It was an analytical jumping off point that could be altered with empirical methods (Begley and Landes 1973). Kirk and Dodds used the original J integral as a measurement of strain energy in the elastic region;

they then added the estimation formula, in the geometrically independent form of plastic work, to replace the crude hinge model used in E1290 to describe plastic deformation.

The proposed annex to E1290 takes this later work into consideration. In many ways, it is considered a *refinement* of the current standard, rather than an alternative method. The application to weld material is, as previously explained, particularly applicable in light of material heterogeneity and residual stresses. The use of compression is also aimed at improving weldment calculations.

Details of the equations used in E1290 as well as the proposed annex may be found in Appendix I, Derivation of Equations. This appendix strives to explain the mathematical calculations as well as give further background on their development.

Procedures

The acknowledged goal of this paper is to determine the suitability of the E1290 annex for use. This determination will take a two pronged approach. First, the annex will be compared to the current standard in both calculations and methodology. Second, a series of single-edge notched bend (SENB) tests will be run to evaluate field performance of the annex.

Standard Comparison

The proposed annex to E1290 differs from this standard in calculations as well as procedure.

Calculation changes vary from the theoretical to the empirical. The driving change behind this annex is a theoretical modification that deals with the plastic work equation discussed earlier (Kirk and Dodds 1993). E1290 currently estimates plastic CTOD using a hinge model that relates CMOD and CTOD with similar triangles (see Figure Two and Appendix I for further details). The annex proposes a calculation based on the plastic J integral and the plastic work solution for SENB specimens (Rice, Paris, and Merkle 1973).

This new calculation for the plastic J integral leads to a change in notation. Instead of calculating separate elastic (via the J integral) and plastic (via the hinge model) CTOD components, the annex calculates the entire J integral, both elastic and plastic components. The linear relationship between J and CTOD is then used to obtain a total CTOD value (Shih 1981).

Another notation change appears in the calculation of the stress concentration factor, K . Several terms in the equations for K have been rearranged between E1290 and the annex; however, the numerical value remains identical. Equality of the concentration factors is revealed through simple algebraic manipulation, as shown in Appendix I.

Other differences between the standards concern the use of empirical constants. E1290 uses set constants in its calculations; the annex replaces these constants with equations, obtained through linear regression and other numerical techniques, to more accurately model behavior (Kirk and Wang 1995). Finite element analysis was used for confirmation of these equations.

Procedurally, E1290 and its annex are similar. However, in keeping with its weldment focus, the annex has added local compression to the test sequence. Because of residual stresses in weld metal, it is difficult to create a straight crack face (Dawes, Pisarski, and Squirrel 1989). A straight crack face is important in order to sample a uniform region of material. Because material composition varies regionally in weld metal, a fracture toughness value means little if it samples a material hodge-podge.

Through local compression, residual stresses are relieved and compression stresses are induced. Both of these processes work to create a straight crack face, thus fostering a uniform material sample. Details are discussed further in the next section.

Single Edge Notched Bend Tests

ASTM supplied three sections of circular, welded pipe. Specimen blanks were machined from this pipe. The specimens were approximately four inches long with a depth and width of one inch and were notched to a depth of approximately 0.36 inches. Notches were placed in the center of the weld metal and ran parallel to the weld length.

Figure Three illustrates this configuration, and dimensions of each specimen are summarized in Table One.

In order to ensure a straight crack face, ASTM requires local compression of the notched weld region. A test fixture was machined to aid in this compression. The fixture was U-shaped and laid on its side, the arms of the U forming the top and bottom. Circular holes, half an inch in diameter, were cut in the arms of this fixture. Into these holes fit half-inch cylindrical platens. The specimen being compressed fit into this fixture so that the holes covered the tip of the notch. The platens were then loosely inserted into the holes. This configuration, shown in Figure Four, was placed into a MTS 110 kip load frame; loads, calculated using specimen size and material strength, were applied until the requisite one percent width reduction was obtained. (ASTM supplied material property data via the Idaho National Engineering and Environmental Laboratory; see Table Two.)

The sacrifice specimen was then placed into a 22 kip MTS load frame where it underwent fatigue loading. The loading cycle during fatigue was controlled first using a user-defined VI program and then using a MTS 410 digital function generator. Loads were again kept within ranges dictated by size and strength. Fatiguing caused a crack to grow from the tip of the specimen notch. When this crack reached a depth of approximately 0.70 inches, including notch depth, fatiguing stopped.

The cracked specimen was immersed in liquid nitrogen until cooled to the temperature of this medium; once cold, it was placed into the 22 kip machine and loaded until failure. A nine-point average of the crack depth was taken from the crack surface of the broken specimen. To qualify as a straight crack face, shown in ideal form in Figure Five, none of these nine measurements may differ from the average crack depth value by

more than 20 %. Once an acceptably straight crack face was established, the remaining specimens could be tested.

The bend specimens underwent the same compression and fatiguing process as the sacrifice specimen. However, these specimens are fatigued only until the crack depth reaches approximately 0.50 inches. (This depth varies by specimen; ASTM requires a crack depth within 45 – 55 % of specimen width.)

Having been fatigued, the ambient temperature specimens were bent in a MTS 55 kip load frame. Loading is arranged as shown in Figures Six and Seven. The specimen deforms as load increases. A computer monitors load, time, and crack-mouth opening displacement (CMOD) through the use of a clip gauge placed at the notch opening. When critical crack extension or load plateau is accomplished, the specimen is unloaded and broken, as previously described with the sacrifice specimen.

The liquid nitrogen specimens differ from those tested at room temperature only in the bending process. Liquid nitrogen was poured into a metal, styrofoam-covered container. An Instron model 1125 test fixture was lowered into the liquid nitrogen so that specimens underwent bending at a temperature of -196° F.

Analysis of the data taken from these specimens will rely upon the following criteria:

- ▶ *Reproducibility*: A specimen tested at room temperature should have a critical CTOD value similar to that of other specimens tested at the same temperature. Likewise, a correlation should be seen between CTOD values of specimens tested at liquid nitrogen temperature. Failure to reproduce these results indicates an arbitrary measure of fracture toughness which can have little to no practical value in the field.

- ▶ *Expected temperature variations:* Theoretically, fracture toughness should decrease with a decrease in temperature (Harrison et al. 1977). Therefore, specimens tested in liquid nitrogen should exhibit more brittle behavior than those tested under ambient conditions. If the critical CTOD values for these specimens do not show this behavioral distinction, there is reason to suspect a flaw in the annex calculations.
- ▶ *Similarity to E1290:* As mentioned earlier, E1290 is suspected of overestimating CTOD (Kirk and Wang 1995). The annex calculations are expected to estimate actual fracture toughness within a 9 % range (Kirk and Dodds 1992). However, E1290 is a valid indication of fracture toughness. Therefore, annex calculations are expected to be lower than those obtained with E1290 but to observe *all other trends* apparent in the standard's calculations.
- ▶ *Local Compression:* Since local compression is a new feature of the annex testing procedure, we must consider whether or not it accomplishes the desired goal. In this case, whether or not local compression produced straighter crack faces.

Results

The first sacrifice specimen had a badly curved crack face. Investigation revealed that the load used during local compression was too small to produce the requisite indentation; load was increased from 24 to 26 kips to satisfy this requirement. Two reserve specimens were used before obtaining an acceptably straight crack face, in part because a laboratory accident prevented examination of specimen two. Table Three shows the points used to find average crack depth and their variation from this average.

Five specimens underwent bending and data analysis. Three of these tests were conducted at ambient temperature and two at liquid nitrogen temperature. Fracture toughness values were obtained for two of the ambient specimens. Bending of the third specimen, L15-3, was mistakenly stopped before completion; therefore, data was incomplete and unusable. However, both liquid nitrogen specimens yielded fracture toughness values. Table Four summarizes critical fracture toughness data; Figures Eight through Eleven show the graphical representation of E1290 and annex CTOD calculations for each of the specimens.

Specimens tested at room temperature were classified as δ_m values. This classification means the CTOD values reach a maximum load plateau before gradually unloading. The specimens bent but did not fracture; they were loaded only until the crack propagated, as was indicated by the load drop.

In liquid nitrogen, the specimens obtained δ_o values. This classification means a point was reached at which the crack not only propagated but fractured the material. Prior to fracture, significant material tearing (greater than 0.008 in) occurred.

Discussion

The fracture toughness data obtained from the bend tests must be evaluated in terms of the criteria set forth earlier.

The first of these requirements was reproducibility. The values calculated at both ambient and liquid nitrogen temperatures showed a strong tendency to agree. There was a less than 5 % difference between the critical values obtained at room temperature. Toughness of the liquid nitrogen specimens also agreed, with a larger percent difference of roughly 20 %. However, values for these same specimens obtained through E1290 calculations differed by 25 %. Therefore, it appears that the annex can reproduce toughness values for similar specimens under similar conditions, at least to the degree of accuracy present in E1290.

Secondly, the annex was expected to show temperature variations. The specimens tested at room temperature, roughly 72° F, exhibited higher critical CTOD values than did the specimens tested in liquid nitrogen. At warmer temperatures, the cracks were more likely to blunt before propagating; at colder temperatures, the specimens behaved in a brittle manner. The Risk Matrix of Canadian Offshore Structures Standard classifies a CTOD value of 0.0028 inches at application temperature to have good control over crack initiation and fair-to-good crack arrest toughness (Lampman 1996). According to this standard, the steel tested would be moderately tough at room temperature and decidedly brittle in liquid nitrogen. By exhibiting a change from tough to brittle behavior, the test specimens behaved as expected, as did the annex calculations.

Of course, the values obtained by the annex must also resemble the values of E1290. Differences of around 10 % existed between the calculations for room temperature specimens. For the liquid nitrogen temperatures, the CTOD differences were smaller, roughly 2 – 3 %. In both cases, the critical annex value was smaller than the E1290 value. Since E1290 theoretically overestimates CTOD, the annex behaved as was expected.

Lastly, the success of local compression in obtaining a straight crack face must be considered. The original sacrifice specimen failed to reach the indentation required by the annex; when fatigued, this specimen also failed to meet straightness criteria. Once the compression load created the proper level of indention, the third sacrifice specimen did meet specimen standards. As shown in Table Three, all nine points used to determine average crack depth of the sacrifice specimen fell within 20 % of this average value, with the largest variation being 17 %. Furthermore, the four specimens tested met this criteria with only one specimen having a maximum variation over 12 %. Sufficient compression caused a *marked change from unacceptable to acceptable* crack straightness; this occurrence tends to corroborate the annex's assertion that local compression will produce straighter cracks in weld material.

However, it is important to note that the compression load, calculated from specimen geometry and material strength data, was *insufficient* to produce the full 1 % width reduction desired. Local compression was not successful until this load was increased beyond the calculated value. It is unclear whether the load was miscalculated due to material strength misinformation or a fault in the equation used. Either way, the

mechanics of local compression should be further studied before publication of the final standard.

Before drawing any conclusions, a few relevant facts should be discussed. First, ASTM requires a minimum of three successful tests to verify the critical CTOD of a specimen. Only two fracture toughness values were obtained for specimens at both temperatures tested. However, the critical CTOD values for these specimens closely resembled each other. E1290 calculations were another source of confirmation.

Also, fatigue crack growth was monitored visually due to the unpredictable behavior of the material. This method of controlling crack growth is a possible source for error since crack depth in the center of the weld could not be determined. None the less, this method allowed detection of uneven crack growth. This observation led to the discovery that some of the specimen cross-sections were not perfectly square. During the fatigue cycle, the taller side of the specimen received a greater load distribution and began to crack earlier. The specimen could then be realigned so that the load was evenly distributed and cracks would grow at a more even rate; some experimentation was required before this procedure was sufficiently mastered.

Another problem manifested itself in the CMOD data obtained from the liquid nitrogen specimens, particularly for R2-4. Time steps are uneven and unexpected jumps in load and CMOD occur. This unusual data set therefore yields CTOD values with more scatter than normally calculated.

Overall, the annex produced critical CTOD values that were reproducible, representative of expected temperature variations, and similar to E1290 calculations. Local compression was successful in creating a straighter crack front.

Conclusions

The proposed annex to ASTM E1290-93 appears to successfully model the behavior of single edge notched bend specimens tested. The critical crack-tip opening displacements meet requirements of reproducibility, temperature variation, and similarity to the current standard. The technique of local compression also generated a straighter crack face.

The proposed annex is more desirable than the current standard theoretically because it uses work to obtain the plastic portion of CTOD, rather than a geometrical model which assumes a dubious linear relationship with CMOD. The annex is also more desirable experimentally, as the values obtained show less tendency to scatter.

Although further experimental verification is warranted, as well as an examination of the methods used to determine compression loads, current evidence suggests that the proposed annex is a reliable fracture toughness measure for structural weldments. ASTM should favor adoption of this standard.

The importance of fracture toughness cannot be sufficiently stressed. While this property has proved hard to quantify in the past, it remains an important element in material behavior. Flaws are inevitable in the construction of any structural component. If we do not know how a component will behave once flawed, then we cannot ensure the safety and reliability of that component.

Fracture toughness takes on special significance for welded materials. The welding process introduces material heterogeneity and residual stresses, both of which will affect, even alter, material behavior. Use of low toughness material can undermine an

otherwise sound design, as was illustrated by the girder-column building failures in both the Kobe, Japan, and Northridge, California, earthquakes of the mid-nineties. In these instances, critical welded joints severed under lateral loading conditions. These weldments, used because of steel's ductility and ability to deform without breaking, behaved in exactly the sort of brittle fashion they were designed to prevent. A simple laboratory procedure may have predicted this behavior.

This paper has presented and analyzed a particularly useful measure of fracture toughness in the form of crack-tip opening displacement. CTOD holds many advantages over other toughness parameters, particularly in its abilities to model both elastic and plastic behavior and be integrated into finite element analysis of structural designs. The new method for calculating CTOD presented in the proposed annex to ASTM E1290-93 meets behavioral expectations and answers several theoretical criticisms of the current standard.

The new method for determining CTOD conforms to the high quality expectations demanded of an ASTM standard. Adoption of this annex will improve current measurement of fracture toughness and further advance the critical study of fracture mechanics.

Acknowledgements

I wish to extend my gratitude to the following individuals who have aided me in my examination of the E1290 annex.

To Harold Reemsnyder, for providing me with sample test data used to develop a program for performing both the annex and E1290 calculations.

To Andrew Fawcett, director of the Testing Measurement and Research Facility, for his assistance and instruction in performing all aspects of the testing procedure, and also for his patience during this process.

To Dr. Gary Fry, for his insight, instruction, and guidance in all stages of this experiment, from proposal to thesis, and for his ability to remain sane throughout.

References

- Anderson, T. L. *Fracture Mechanics: Fundamentals and Applications*. Boca Raton: CRC Press, 1995. Textbook for basic principles in fracture mechanics. Derives many of the equations used in CTOD calculations, among others. Explains basic fracture toughness, mechanics concepts.
- American Society for Testing and Materials. *1995 Annual Book of ASTM Standards*. Philadelphia: American Society for Testing and Materials, 1995. Provided a copy of ASTM E1290-93 as well as other standards.
- Bilby, B. A., K. J. Millar, and J. R. Willis (ed). *Fundamentals of Deformation and Fracture*. Cambridge: Cambridge University Press, 1985. The introduction of this book presents a memorial look at Eshelby's life and work on energy momentum tensor.
- Begley, J. A. and J. D. Landes. "A Comparison of J Integral Fracture Criterion with Equivalent Energy Concept." In *Progress in Flaw Growth and Fracture Toughness Testing*. ASTM STP 536. Philadelphia: ASTM, 1973. Discusses J integral as expansion of linear elastic fracture mechanics.
- Begley, J. A. and J. D. Landes. "The J Integral as a Fracture Criterion." In *Fracture Toughness*. ASTM STP 514. Philadelphia: ASTM, 1972. Supports the J integral as a fracture toughness parameter and discusses its advantages of K and CTOD.
- Begley, J. A. and J. D. Landes. "Recent Developments in J_{IC} Testing." In *Developments in Fracture Mechanics Test Methods Standardization*, edited by W. F. Brown, Jr. and J. G. Kaufman. ASTM STP 632. Maryland: ASTM, 1977.

- Bucci, R. J., B. N. Greene, and P. C. Paris. "Fatigue Crack Propagation and Fracture Toughness of 5 Ni and 9 Ni Steels at Cryogenic Temperatures." In *Progress in Flaw Growth and Fracture Toughness Testing*. ASTM STP 536. Philadelphia: ASTM, 1973. Examines relationship between flaws, fracture, and critical size.
- Dawes, Michael G. "Elastic-Plastic Fracture Toughness Based on the COD and J-Contour Integral Concepts." In *Elastic-Plastic Fracture* edited by J. D. Landes, J. A. Begley, and G. A. Clarke. ASTM STP 668. Baltimore: ASTM, 1977. Presents history of CTOD development.
- Dawes, Michael G., Henryk G. Pisarski, and Stephen J. Squirrel. "Fracture Mechanics Tests of Welded Joints." In *Nonlinear Fracture Mechanics: Elastic-Plastic Fracture*. ASTM STP 995. Philadelphia: ASTM, 1989. Presents various uses for fracture toughness assessments, especially for weldments, as well as some problems in determining weldment toughness.
- Dugdale, D. S. "Yielding of Steel Sheets Containing Slits." *Journal of Mechanics and Physical Solids* (1960): 100-104. The original account of Dugdale's strip model for plastic deformation.
- Glinka, Grzegorz. "Effect of Residual Stresses on Fatigue Crack Growth in Steel Weldments Under Constant and Variable Amplitude Loads." In *Fracture Mechanics* edited by C. W. Smith. ASTM STP 677. Maryland: ASTM, 1979. Discusses effects of residual stresses on weldment measurements.
- Harrison, J. D., M. G. Dawes, G. L. Archer, and M. S. Kamath. "The COD Approach and Its Application to Welded Structures." In *Elastic-Plastic Fracture* edited by

J. D. Landes, J. A. Begley, and G. A. Clarke. ASTM STP 668. Baltimore: ASTM, 1977. Discusses use of CTOD curve and its development.

Hellan, Kare. *Introduction to Fracture Mechanics*. New York: McGraw-Hill Book Company, 1984. Basic fracture mechanics textbook. Explains crack propagation and derives proofs for equations used.

Imhoff, E. J. and J. M. Barsom. "Fatigue and Corrosion-Fatigue Crack Growth of 4340 Steel at Various Yield Strengths." In *Progress in Flaw Growth and Fracture Toughness Testing*. ASTM STP 536. Philadelphia: ASTM, 1973. Discusses reasons behind material fracture.

Iwankiew, Nestor R. and Charles J. Carter. "The Dogbone: A New Idea to Chew On." *Modern Steel Construction* (April 1996): 18-23. Details problems related to weldment failure in earthquakes.

Irwin, G. R. "Analysis of Stresses and Strains Near the End of a Crack Traversing a Plate." *Journal of Applied Mechanics* (1957): 361-364. Promotes use of Griffith theory for metals; discusses changes in fracture mechanics and motivation behind them.

Joh, Changbin and W. F. Chen. "Application of Fracture Mechanics to Steel Connections in Moment Frame Under Seismic Loading." In *Advances in Structural Engineering*. United Kingdom: Multi-Science Publishing Company Limited, 1997. Discusses problems with weldment failures.

Kirk, M. T. and R. H. Dodds, Jr. "Experimental J Estimation Formulas for Single Edge Notch Bend Specimens Containing Mismatch Welds." In *Materials Engineering. Offshore Mechanics and Arctic Engineering- 1992*, vol. 3-B. New York: ASME,

1992. Proposes and compares error between two new J integral calculations (one of which was later used in Annex).
- Kirk, M. T. and R. H. Dodds, Jr. "J and CTOD Estimation Equations for Shallow Cracks in Single Edge Notch Bend Specimens." *Journal of Testing and Evaluation* (1993): 228-238. Proposal of plastic work inclusion in J integral.
- Kirk, M. T. and Y-Y. Wang. "Wide Range CTOD Estimation Formulae for Single Edge Bend Specimens." In *Fracture Mechanics*. ASTM STP 1256. Philadelphia: ASTM, 1995. Correlates data from previous experiments and proposes equations to model constants.
- Lampman, Steven R. (ed). *ASM Handbook: Fatigue and Fracture*. USA: ASM International, 1996. Provided CTOD requirements for moderately tough material.
- "Magnitude 6.7 Northridge, California, Earthquake of 17 January 1994." *Science* (21 October 1994): 389-397. Describes aftermath of Northridge earthquake.
- Nelson, F. G. and J. G. Kaufman. "Fracture Toughness of Plain and Welded 3-Inch-Thick Aluminum Alloy Plate." In *Progress in Flaw Growth and Fracture Toughness Testing*. ASTM STP 536. Philadelphia: ASTM, 1973. Discusses fracture toughness values in weld metal and problems with calculations thereof.
- Normile, Dennis. "A Wake-Up Call from Kobe." *Popular Science* (February 1996): 64-68. Describes aftermath of Kobe earthquake.
- Paris, P. C., H. Tada, Z. Zahor, and H. Ernst. "Instability of the Tearing Mode of the Elastic-Plastic Crack Growth." In *Fundamentals of Deformation and Fracture* edited by B. A. Bilby, K. J. Millar, and J. R. Willis. Cambridge: Cambridge University Press, 1985. Supported J integral as a measurement of crack instability.

- Rice, J. R. "Conservative Integral and Energetic Forces." In *Fundamentals of Deformation and Fracture* edited by B. A. Bilby, K. J. Millar, and J. R. Willis. Cambridge: Cambridge University Press, 1985. Discusses Eshelby's work on elastic integral, comparison to elastic-plastic J integral and deformation theory.
- Rice, J. R. "A Path Independent Integral and the Approximate Analysis of Strain Concentration by Notches and Cracks." *Journal of Applied Mechanics* (1968): 379-386. Original derivation for path independence of J integral and conditions near the crack-tip.
- Rice, J. R., P.C. Paris, and J. G. Merkle. "Some Further Results of J Integral Analysis and Estimation." In *Progress in Flaw Growth and Fracture Toughness Testing*. ASTM STP 536. Maryland: ASTM, 1973. Proposes geometry specific solutions of J integral for common test specimens.
- Robinson, J. N. and A. S. Tetelman. "Measurements of K_{IC} on Small Specimens Using Critical CTOD." In *Progress in Flaw Growth and Fracture Toughness Testing*. ASTM STP 536. Maryland: ASTM, 1973. Discusses procedure for measuring CTOD using silicone rubber impressions.
- Rolfé, Stanley T. and John M. Barsom. *Fracture and Fatigue Control in Structures: Applications of Fracture Mechanics*. New Jersey: Prentice-Hall Incorporated, 1977. Relates early history of fracture mechanics.
- Rooke, D. P. "Development of Fracture Mechanics." In *Static and Dynamic Fracture Mechanics*, edited by M. H. Aliabadi, C. A. Brebbia, and V. Z. Parton. Massachusetts: Computational Mechanics Publications, 1994. Gives history and background information on fracture mechanics.

- Shang-Xian, Wu. "Plastic Rotational Factor and J-COD Relationship of Three Point Bend Specimen." *Engineering Fracture Mechanics* (1983): 83-95. Discusses methods of calculating J and CTOD.
- Shih, C.F. "Relationship between the J integral and the Crack Opening Displacement for Stationary and Extending Cracks." *Journal of the Mechanics and Physics of Solids* (1981): 305-326. Proposes linear relationship between J and CTOD; corroborates for work hardened materials.
- Shih, C. F. and Hutchinson, J. W. "Fully Plastic Solutions and Large-Scale Yielding Estimates for Plane Stress Crack Problems." *Journal of Engineering Materials and Technology* (1976): 289-295. Asserts accuracy of J integral for fully plastic behavior.
- Sih, G. C. "Fracture Toughness Concept." In *Properties Related to Fracture Toughness*. ASTM STP 605. Philadelphia: ASTM, 1976. Discussion of fracture toughness and its use in industry.
- Underwood, J. H. " J_{IC} Results and Methods with Bend Specimens." In *Fracture Mechanics* edited by C. W. Smith. ASTM STP 677. Maryland: ASTM, 1979. Discusses J integral as an estimation procedure.
- Xue, Ming, Eric J. Kaufman, Le-We Lu, and John W. Fisher. "Achieving Ductile Behavior of Moment Connections—Part II." *Modern Steel Construction* (1996). Describes behavior of weldments in Northridge and Kobe earthquakes.

Tables

Table One: Specimen Dimensions

Specimen Designation	Test Details	Width (in)	Thickness (in)	Length (in)	Notch Depth (in)	Crack Depth (in)
C14-5	Sacrifice	1.003	1.000	4.254	0.360	----
L15-5	Sacrifice	1.003	1.001	4.258	0.354	----
R2-2	Sacrifice	0.970	0.974	4.258	0.351	0.7046
L15-4	Liquid Nitrogen	0.995	1.003	4.259	0.356	0.5578
L15-3	Ambient	1.002	1.000	4.253	0.360	----
R2-1	Ambient	0.971	0.970	4.256	0.353	0.5403
R2-4	Liquid Nitrogen	0.970	0.974	4.253	0.351	0.5310
C14-1	Ambient	0.995	1.000	4.253	0.359	0.5766

Specimens listed in test sequence.

Table Two: Material Properties

Material Property	Ambient Specimens (MPa)	Liquid Nitrogen Specimens (MPa)
<i>Ultimate Tensile Strength</i>	593	989
<i>0.2 % Yield Strength</i>	548	888
<i>Flow Strength</i>	571	939
<i>Elastic Modulus</i>	205,944	218,392

Data supplied by Idaho National Engineering and Environmental Laboratory.

Table Three: Crack Straightness Data

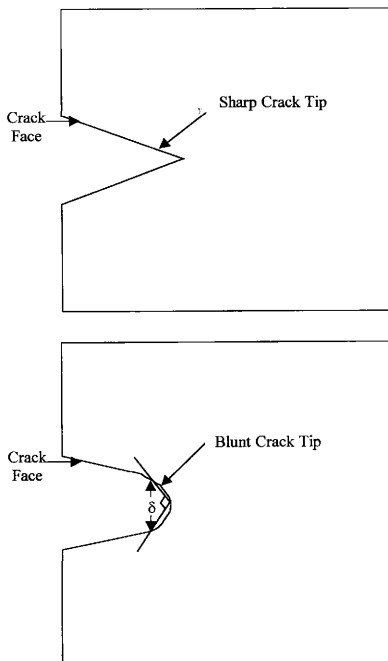
Remaining Ligament (in)	Final Crack Depth (in)	Differs From Average (%)
0.293	0.681	3.35
0.276	0.698	0.94
0.266	0.708	0.48
0.262	0.712	1.05
0.255	0.719	2.04
0.253	0.721	2.33
0.263	0.711	0.91
0.283	0.691	1.93
0.392	0.582	17.40

Average crack depth = 0.7046 in.

Maximum variation = 17 %

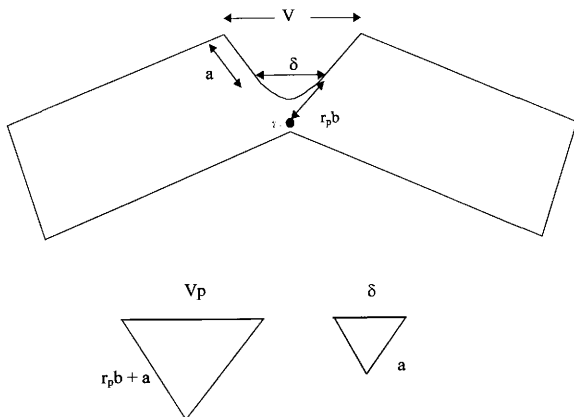
Table Four: Critical Fracture Toughness Data

Specimen	Annex CTOD (in)	E-1290 CTOD (in)	Percent Difference
R2-1 (72° F)	0.0151	0.0171	11.7 %
C14-1 (72° F)	0.0157	0.0172	8.8 %
R2-4 (-196° F)	0.00019	0.00020	2.4 %
L15-4 (-196° F)	0.00024	0.00024	2.4 %

Figures**Figure One: Crack-Tip Opening Displacement Definition**
(Based on picture in Anderson 1995)

δ = Crack-Tip Opening Displacement, CTOD

Figure Two: Similar Triangles Analysis

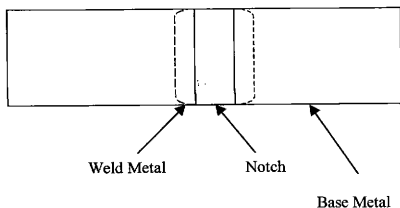


Variable Definitions

W = specimen width
 P = applied load
 V_p = plastic crack-mouth opening displacement (CMOD)
 δ = crack-tip opening displacement (CTOD)
 a = original crack depth
 r_p = plastic rotational factor
 b = uncracked ligament = $W - a$

Figure Three: Specimen Configurations
(Figure drawn to scale.)

Top View



Side View

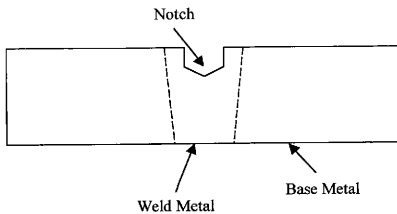


Figure Four: Compression Fixture
(Figure not drawn to scale.)

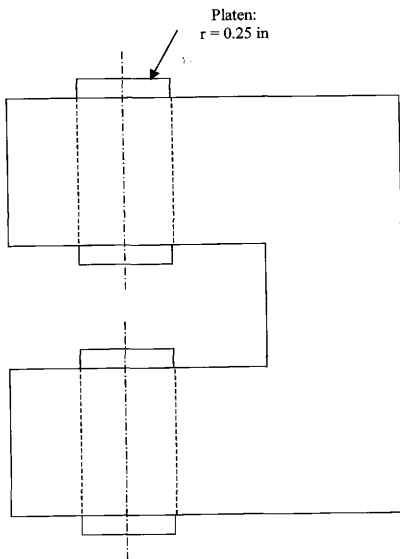


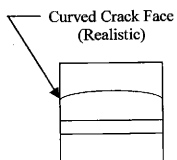
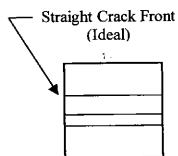
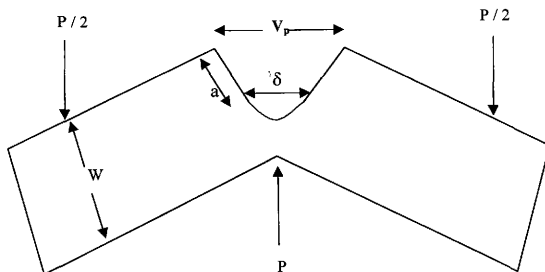
Figure Five: Straight vs. Realistic Crack Faces

Figure Six: Schematic of Specimen Loading**Variable Definitions**

W = specimen width

P = applied load

V_p = plastic crack-mouth opening displacement (CMOD)

δ = crack-tip opening displacement (CTOD)

a = original crack depth

Figure Seven: Single Edge Notch Bend Test

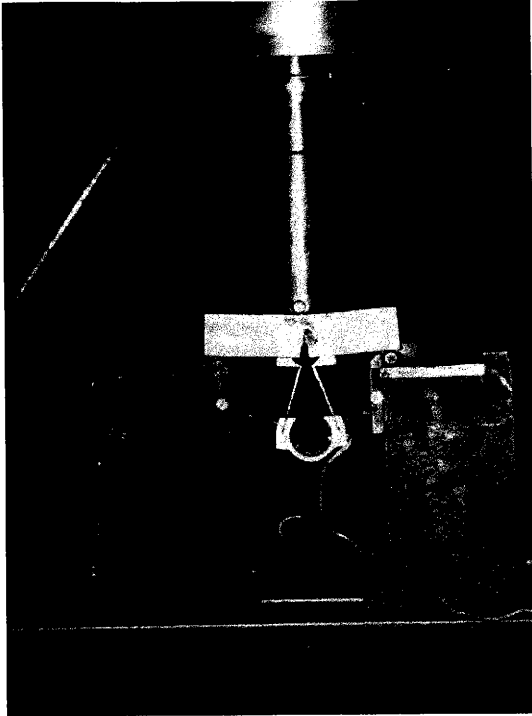
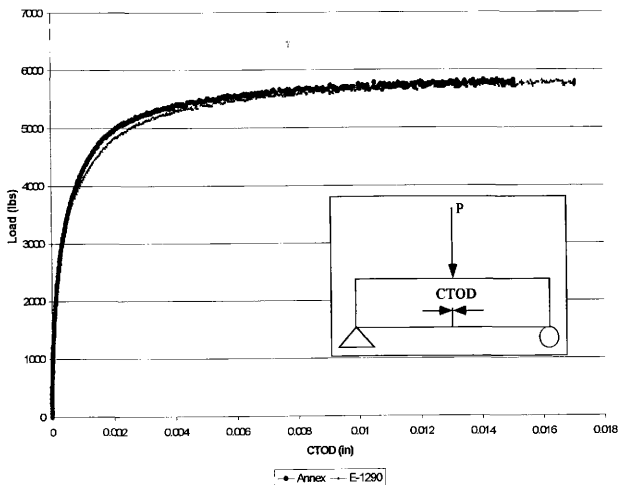


(Figure undergoes loading and starts to bend. Clip gauge placed at specimen mouth measures crack mouth opening displacement.)

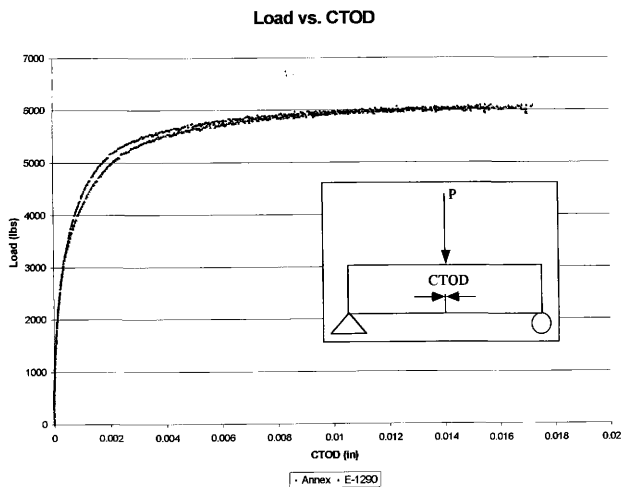
Figure Eight: R2-1 Results
Tested at 72° F

Load vs. CTOD



Critical CTOD:
Annex = 0.0151 in
E-1290 = 0.0171 in

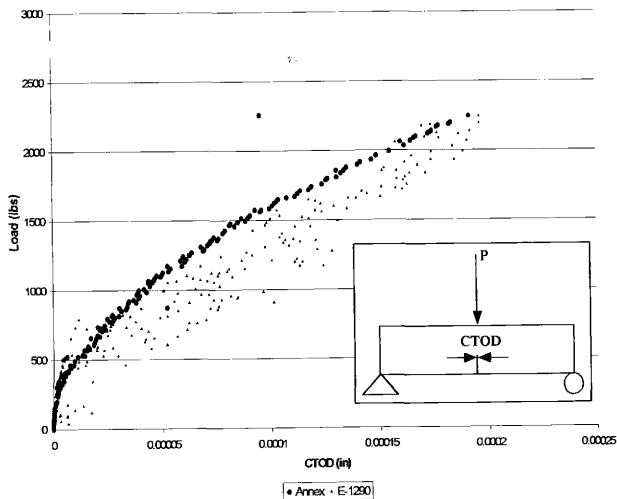
Figure Nine: C14-1 Results
Tested at 72° F



Critical CTOD:
Annex = 0.0157 in
E-1290 = 0.0172 in

Figure Ten: R2-4 Results
Tested at -196°F

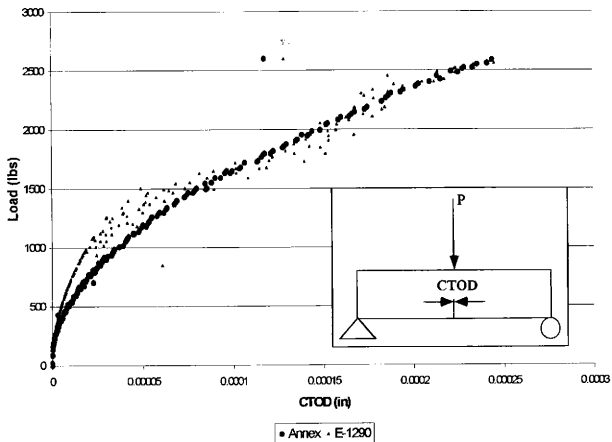
Load vs. CTOD



Critical CTOD:
Annex = 0.000191 in
E-1290 = 0.000196 in

Figure Eleven: L15-4 Results
Tested at -196°F

Load vs. CTOD



Critical CTOD:
Annex = 0.000191 in
E-1290 = 0.000196 in

Appendix I: Derivation of Equations

The following analysis details calculations for both ASTM E1290-93 and its proposed annex. An effort was made to explain the mathematical derivation, rather than the historical outline provided in the Literature Review.

Variables

The equations used to calculate crack-tip opening displacement (CTOD) in ASTM E1290-93 and the proposed annex to this standard require the following variables:

<i>Symbol</i>	<i>Name</i>	<i>Units</i>
δ	crack-tip opening displacement (CTOD)	in
V_p	plastic component crack-mouth opening displacement (CMOD) obtained from clip gauge readings	in
η_c	proportionality constant	dimensionless
n	work hardening coefficient	dimensionless
m	proportionality constant	dimensionless
K	stress concentration factor	psi
J	J contour integral	lb(f)/in
P	load	lb
S	unsupported span of specimen	in
W	width of specimen	in
a	original crack length	In
b	remaining ligament, $b = w - a$	in
B	base of specimen	in
A_c	area under load vs. plastic CMOD plot	lb(f)-in
σ_n	flow strength of weld; average of ultimate tensile strength and yield strength	psi
$f(a/w)$ or Y	proportionality constant	dimensionless
ν	Poisson's ratio	dimensionless
σ_{YS}	yield strength of base metal	psi
z	distance from knife edge measurement point from front face (notched surface)	in
r_p	plastic rotation factor	dimensionless
E	modulus of elasticity	psi

Other variables will be defined as needed.

E1290

ASTM E1290-93 uses the following equations to calculate CTOD:

$$(1) \delta = K^2 (1 - \nu^2) / 2\sigma_{YS}E + r_p b V_p / (r_p b + a + z)$$

$$(2) K = YP / (BW^{1/2})$$

$$(3) Y = \frac{6(a/W)^{1/2} (1.99 - a/W [1 - a/W] [2.15 - 3.93a/W + 2.7(a/W)^2])}{(1 + 2a/W)(1 - a/W)^{3/2}}$$

Equation (1) contains both a plastic and an elastic component. The elastic portion, $K^2 (1 - \nu^2) / 2\sigma_{YS}E$, is obtained by applying Linear Elastic Fracture Mechanics.

The J contour integral is a line integral that represents the energy release rate in a cracked, nonlinear elastic body (Anderson 1995). This definition of J parallels that of the crack driving force, G, for a linear elastic body but allows J to model elastic-plastic deformation (Bilby 1985). When this substitution occurs, J is no longer valid as the energy release rate but as a parameter characterizing stress intensity near the crack-tip deformation field (Rice 1985).

From the theory of elasticity, we know that the crack driving force, G, relates to the stress concentration, K, caused by the specimen notch and original crack. The test apparatus restrains deformation in the SENB specimen and fulfills the conditions for plane strain. For a body in plane strain, the following relationship applies (Hellan 1984):

$$\triangleright G = K^2 (1 - \nu^2) / E$$

For the elastic-plastic model, this elastic relationship becomes:

$$(4) J_{el} = K^2 (1 - \nu^2) / E$$

Substituting this J value into the elastic portion of equation (1) allows the following simplification:

$$\triangleright \delta = J / 2\sigma_{YS}$$

A more careful examination of J corroborates this simplification. For a material of area Γ and an arc length s with negligible body forces, J is mathematically defined by the integral (Hellan 1984):

$$\bullet \quad J = \int_{\Gamma} (w \, dy - t_i \, du_i/dx \, ds)$$

In this instance, w stands for the work of deformation (or strain energy density); t_i and u_i are the traction and crack displacement vectors, respectively. According to Green's theorem, taking the divergence of this line integral transforms it to cover the area inside the curve, A , in the following manner (Anderson 1995):

$$\bullet \quad J = \int_A [dw/dx - \partial/\partial x_i (\sigma_{ij} \partial u_i/\partial x)] \, dx dy$$

The work of deformation can be redefined in terms of the stress tensor, σ_{ij} , and the strain tensor, ϵ_{ij} . As shown below, through a small deformation, ϵ (Anderson 1995):

$$\bullet \quad w = \int_{\epsilon} \sigma_{ij} \epsilon_{ij}$$

Making this substitution and performing some mathematical "clean-up", the J integral becomes (Rice 1968):

$$\bullet \quad J = \int_A [\partial/\partial x_i (\sigma_{ij} \partial u_i/\partial x) - \partial/\partial x_i (\sigma_{ij} \partial u_i/\partial x)] \, dx dy$$

Therefore, the J integral sums to zero along any closed curve Γ , which ensures J 's path independence (Rice 1968). Due to this path independence, we may choose a curve for our J integral that gives the best computational advantage (Hellan 1984). If we take Γ near the tip of the specimen's notch, the integral depends only on the local stress field (Rice 1968). This path makes the traction vector meaningless and reduces the equation to the following:

$$\bullet \quad J = \int_{\Gamma} w \, dy$$

Proximity to the notch means Γ remains within the crack's yield zone (Rice 1968). Because of the specimen loading, the only pertinent stress component is σ_{yy} . According to the strip yield model, $\sigma_{yy} = \sigma_{YS}$ within the yield zone (Anderson 1995). If a represents the original crack and Δa represents the crack growth, the J integral becomes:

$$\bullet \quad J = \int_a^{a+\Delta a} \sigma_{YS} \partial u_2 / \partial x \, dx$$

The displacement u_2 can be taken as a measure of CTOD. Changing variables yields (Anderson 1995):

$$\bullet \quad J = \int_0^\delta \sigma_{YS} \, d\delta$$

Finally, we perform the integration which confirms the previous statement:

$$(5) \quad \delta = J/m\sigma_{YS}$$

The constant m depends on the stress state and material properties of the specimen (Anderson 1995). SEN(B) specimens use $m = 2$ to model the linear elastic portion of the CTOD (Anderson 1995).

Now we examine the stress concentration factor, K . There is a generic K solution which is made specific by the geometry of the specimen. Since geometry is constant, solutions exist for common specimens. These solutions follow the format (Anderson 1995):

$$\bullet \quad K = YP / (BW^{1/2})$$

The function Y is the geometry dependent element. For a SEN(B) specimen, we use the following function (Anderson 1995):

$$\bullet \quad Y = \frac{3S/W (a/W)^{1/2} (1.99 - a/W [1 - a/W] [2.15 - 3.93a/W + 2.7(a/W)^2])}{2 (1 + 2a/W) (1 - a/W)^{3/2}}$$

Substituting $4W$ for S (as dictated by the standard) results in the function:

$$\triangleright Y = \frac{6 (a/W)^{1/2} (1.99 - a/W [1 - a/W] [2.15 - 3.93a/W + 2.7(a/W)^2])}{(1 + 2a/W) (1 - a/W)^{3/2}}$$

This derivation explains equations (2) and (3).

The plastic portion of equation (1), $r_p b V_p / (r_p b + a + z)$, requires less explanation. It is based on a relationship between similar triangles. We assume that the specimen halves are rigid and rotate about a set hinge point (Anderson 1995). The distance between the hinge point and the crack tip is proportional to the length of the uncracked ligament, b . J. D. G. Sumpter derived the constant of proportionality, the so-called plastic rotation factor, based on a limit load analysis of the SEN(B) specimen (Kirk and Dodds 1992). The factor r_p is a function of a/W . Results vary according to the depth of the initial crack; for the range of a/W values permitted by E1290, r_p is commonly taken as 0.44.

V_p , the plastic crack-mouth-opening displacement (CMOD), forms the base of the larger triangle. Figure Two illustrates the similar triangles argument. The length of the sides equals the original crack depth, a , and the distance to the hinge point, $r_p b$. We would also add the offset height of the clip gauge, z , if it did not fit exactly into the specimen. The smaller triangle base is the CTOD. The length of the sides is simply $r_p b$. Therefore, we make the following proportionality:

$$\triangleright \frac{\delta}{r_p b} = \frac{V_p}{r_p b + a + z}$$

Solving this equality for δ give us the following equation:

$$\triangleright \delta = \frac{r_p b * V_p}{r_p b + a + z}$$

We add this factor to equation (1) to complete the CTOD calculation for E1290.

Annex

Now that we have explained the equations used in ASTM E1290, we focus on the equations for the proposed annex.

$$(1) \delta = J/m\sigma_n$$

$$(2) J = K^2(1 - v^2) / E + \eta_c A_c / Bb$$

$$(3) K = PS / (BW^{3/2}) * f(a/W)$$

$$(4) m = 1.221 + 0.793(a/W) + 2.751n - 1.418n(a/W)$$

$$(5) \eta_c = 3.785 - 3.101(a/W) + 2.018(a/W)^2$$

$$(6) n = 1.724 - 6.098/R - 8.326/R^2 - 3.065/R^3$$

$$(7) f(a/W) = \frac{3(a/W)^{1/2}(1.99 - a/W[1 - a/W][2.15 - 3.93a/W + 2.7(a/W)^2])}{2(1 + 2a/W)(1 - a/W)^{3/2}}$$

We have already examined equation (1) and the first part of equation (2) in the previous section. However, the annex makes a few alterations to these calculations.

Equation (1) replaces the yield strength with flow strength, σ_n . Recall that yield strength was appropriate when considering only the elastic yield region. Flow strength represents the average value of yield strength and ultimate tensile strength and helps generalize previous results.

Also in equation (1), m is determined by a polynomial instead of a fixed constant. Kirk and Dodds (1992) used finite element analysis to improve the accuracy of their calculations and find more accurate constants. Later, their results were analyzed and fitted with least square regressions. These regressions produced equation (4) and equation (5) (Kirk and Wang 1995).

The stress concentration factor, although it appears to change, is the same as in E1290. As before, we expect the following relationships (Anderson 1995):

$$\begin{aligned} \blacktriangleright K &= P / (BW^{1/2}) * f(a/W) \\ \blacktriangleright f(a/W) &= \frac{3S/W (a/W)^{1/2} (1.99 - a/W [1 - a/W] [2.15 - 3.93a/W + 2.7(a/W)^2])}{2 (1 + 2a/W) (1 - a/W)^{3/2}} \end{aligned}$$

The Annex nomenclature differs from the pattern, but the answers are mathematically equal. Substituting the expression $f(a/W)$ into the expected stress concentration, we make the following simplifications:

$$\begin{aligned} \blacktriangleright K &= \frac{3PS/W (a/W)^{1/2} (1.99 - a/W [1 - a/W] [2.15 - 3.93a/W + 2.7(a/W)^2])}{2 B W^{1/2} (1 + 2a/W) (1 - a/W)^{3/2}} \\ \blacktriangleright K &= \frac{3PS (a/W)^{1/2} (1.99 - a/W [1 - a/W] [2.15 - 3.93a/W + 2.7(a/W)^2])}{2 B W^{1/2} W (1 + 2a/W) (1 - a/W)^{3/2} (BW^{1/2})} \\ \blacktriangleright K &= \frac{3PS (a/W)^{1/2} (1.99 - a/W [1 - a/W] [2.15 - 3.93a/W + 2.7(a/W)^2])}{2 B W^{3/2} (1 + 2a/W) (1 - a/W)^{3/2} (BW^{1/2})} \end{aligned}$$

Substituting equation (7) into equation (3) yields identical results:

$$\begin{aligned} \blacktriangleright K &= \frac{PS}{BW^{3/2}} * \frac{3(a/W)^{1/2} (1.99 - a/W [1 - a/W] [2.15 - 3.93a/W + 2.7(a/W)^2])}{2 (1 + 2a/W)(1 - a/W)^{3/2}} \\ \blacktriangleright K &= \frac{3PS (a/W)^{1/2} (1.99 - a/W [1 - a/W] [2.15 - 3.93a/W + 2.7(a/W)^2])}{2 B W^{3/2} (1 + 2a/W) (1 - a/W)^{3/2} (BW^{1/2})} \end{aligned}$$

Remembering that E1290 specifications require a span of $4W$, we find that the Annex stress concentration has not changed from the one used in the previous standard.

$$\begin{aligned} \blacktriangleright K &= \frac{3P (4W) (a/W)^{1/2} (1.99 - a/W [1 - a/W] [2.15 - 3.93a/W + 2.7(a/W)^2])}{2 B W^{3/2} (1 + 2a/W) (1 - a/W)^{3/2} (BW^{1/2})} \\ \blacktriangleright K &= \frac{6P (a/W)^{1/2} (1.99 - a/W [1 - a/W] [2.15 - 3.93a/W + 2.7(a/W)^2])}{B W^{1/2} (1 + 2a/W) (1 - a/W)^{3/2} (BW^{1/2})} \end{aligned}$$

Therefore, the elastic portion of equation (2) has not altered in the Annex. For the first time, however, we see a plastic portion of the J integral, which replaces the hinge point model used in E1290.

Previously, we used a line integral as a definition for J; however, a simpler definition for J exists. As we mentioned earlier, J defines the energy release rate for nonlinear elastic materials. The following definition applies for a crack area A (Anderson 1995):

$$\blacktriangleright J = -d\Pi / dA$$

The potential energy, Π , may be further defined in terms of the strain energy, U, and the work done by external forces, F (Anderson 1995). (In fact, this definition merely restates the previously derived result: $J = \int_A [dw/dx - \partial/\partial x_i (\sigma_{ij} \partial u_i / \partial x)] dx dy$.)

$$\blacktriangleright \Pi = U - F$$

For the loading case in question, $F = PV_p$ (Hellan 1984). The strain energy portion of this integral was developed in the previous section to explain J's relationship to K; it is no longer important. In a load controlled situation, the external loading portion of the J integral simplifies to:

$$\blacktriangleright J = \int_p (\partial V_p / \partial A)_p dP$$

$$\blacktriangleright J = PV_p / A$$

The cross sectional area, A, of the uncracked body depends on the base, B, and the remaining ligament, b. Kirk and Dodds (1992) were the first to replace PV_p with the area under the load versus plastic CMOD curve, A_e . However, the "estimation formulas" designed by Rice, Paris, and Merkle actually used a similar formula (Rice, Paris, and

Merkle 1973). The multiplier η_c was added for increased accuracy as explained previously. With these additions, the J integral becomes:

$$\bullet \quad J = \eta_c A_c / Bb$$

Equation (2) is, therefore, the summation of this relationship and the elastic portion of the J contour integral.